

Electronic Structure and Charge Dynamics of Huesler Alloy Fe₂TiSn Probed by Infrared and Optical Spectroscopy

S.V. Dordevic and D.N. Basov

Department of Physics, University of California, San Diego, La Jolla, CA 92093

A. Ślebarski** and M.B. Maple

*Department of Physics and Institute for Pure and Applied Physical Sciences,
University of California, San Diego, La Jolla, CA 92093*

L. Degiorgi

Laboratorium für Festkörperphysik ETH-Zürich, 8093 Zürich, Switzerland

We report on the electrodynamics of a Heusler alloy Fe₂TiSn probed over four decades in energy: from the far infrared to the ultraviolet. Our results do not support the suggestion of Kondo-lattice behavior inferred from specific heat measurements. Instead, we find a conventional Drude-like response of free carriers, with two additional absorption bands centered at around 0.1 and 0.87 eV. The latter feature can be interpreted as excitations across a pseudogap, in accord with band structure calculations.

Fe₂TiSn belongs to a large group of materials commonly referred to as Heusler alloys with the general formula X₂YZ, where X and Y are transition metals and Z is a non-magnetic element. Heusler and closely related half-Heusler (with the formula XYZ) alloys have been the subject of continued interest for almost 70 years¹⁻⁴. A member of this family Fe₂VAl has recently attracted a lot of attention in connection with possible *d*-electron heavy fermion (HF) behavior⁵. The resistivity of Fe₂VAl displayed anomalous temperature dependence and specific heat measurements revealed an upturn in $C_v(T)$ resembling that of conventional *f*-electron HF compounds⁵. However when the specific heat measurements were repeated in high magnetic field they showed that the upturn was due to a Schotky anomaly arising from magnetic clusters, not the Kondo interaction⁶. A number of band structure calculations yield only a minor mass renormalization⁷⁻¹⁰. An infrared (IR) study reported recently for Fe₂VAl (Ref. 11) also finds no characteristic features of the HF state in the electrodynamic response of this compound.

Based on electrical resistivity and specific heat measurements Fe₂TiSn has also been speculated to be a HF metal with the quasiparticle effective mass of $\sim 40 m_e$, where m_e is the free electron mass^{12,13}. Note however that the electronic contribution γ to the specific heat $C_v(T) = \gamma T + \beta T^3$ is relatively small (12 mJ mol⁻¹ K⁻²) compared with conventional HF metals. Moreover, a similar temperature dependence of $C_v(T)$ in Fe₂VAl had first been proposed to be Kondo in origin, and then showed to be due to Schottky anomaly. Motivated by this unsettled issue we used IR and optical spectroscopy to directly test the hypothesis of the HF state in Fe₂TiSn. Optical experiments are perfectly suited for such a task because they probe both the intra- and interband electronic excitations and have been successfully employed in studies of *f*-electron HF systems¹⁴⁻¹⁸.

The polycrystalline samples of Fe₂TiSn were grown by

arc melting under high purity argon on a copper hearth and have previously been characterized by X-ray diffraction, electrical resistivity, susceptibility, specific heat and XPS measurements¹². For IR measurements, the samples were mechanically polished until a mirror-like surface was achieved. Near normal incidence reflectance $R(\omega)$ was measured at UCSD in a broad frequency range 40-20,000 cm⁻¹ (approximately 5 meV - 2.5 eV) and temperature range (from 10 K to 300 K). To obtain the absolute values of $R(\omega)$, the samples were coated in-situ with gold or aluminum in the optical cryostat and the spectrum of a metal-coated sample was used as a reference. This procedure yields reliable absolute values of $R(\omega)$ and does not require ambiguous corrections for diffuse reflectance¹⁹. The IR measurements were supplemented with ultraviolet reflectance measurements up to 100,000 cm⁻¹ (12 eV) performed at room temperature at ETH.

Figure 1 shows the reflectance of Fe₂TiSn at several selected temperatures. The general shape of reflectance is metallic, but the exact position of the plasma minimum is obscured because the free carrier response overlaps with interband transitions. The far-infrared reflectivity ($\omega < 600$ cm⁻¹) decreases as temperature increases, the behavior typical for metallic systems. The mid-infrared reflectance, however, shows more complicated temperature dependence: in the range between 600 - 3,000 cm⁻¹, $R(\omega)$ decreases with temperature. At higher frequencies ($\omega > 3,000$ cm⁻¹), the spectra are temperature independent. The peaks at ~ 250 cm⁻¹ and $\sim 50,000$ cm⁻¹ can be interpreted as an optically active phonon and an interband transition, respectively.

The next step in data analysis is to perform a Kramers-Kronig (KK) transformation on the raw reflectivity data in order to obtain the complex optical conductivity $\sigma(\omega) = \sigma_1(\omega) + i\sigma_2(\omega)$. For the low frequency extrapolation we used a Hagen-Rubens formula, commonly employed for metals: $R(\omega) = 1 - \sqrt{2\omega\rho_{dc}/\pi}$, where ρ_{dc} is the dc resistivity. Several other extrapolations (such as

a straight line or $R(\omega) \sim \omega^2$) produced the same result in the region where the data exist. A power law extrapolation $R(\omega) \sim \omega^{-4}$ was used for high frequencies.

Figure 2 shows the real part of the optical conductivity $\sigma_1(\omega)$. The spectra of Fe_2TiSn are characterized by a Drude-like mode with a width of about 120 cm^{-1} at 10 K and a broad peak centered around $7,000 \text{ cm}^{-1}$ (0.87 eV). As temperature increases, the zero energy peak broadens, whereas the peak at $7,000 \text{ cm}^{-1}$ displays almost no T-dependence. In order to quantify these changes we first employ a conventional Drude-Lorentz model. Fits including a Drude mode and a *single* Lorentzian at $7,000 \text{ cm}^{-1}$ failed to produce satisfactory results. We succeeded in accurately reproducing the ω -dependence of $\sigma_1(\omega)$ at all temperatures with a set of *two* Lorentz oscillators in addition to the Drude term²⁰:

$$\sigma(\omega) = \frac{1}{4\pi} \frac{\omega_p^2 \tau}{1 - i\omega\tau} + \frac{1}{4\pi} \sum_{j=1}^2 \frac{i\omega\omega_{pj}^2}{\omega^2 - \omega_j^2 + i\gamma_j\omega}. \quad (1)$$

The first term represents a Drude free-electron component, where $\omega_p^2 = 4\pi ne^2/m^*$ is the plasma frequency (n is the carrier density and m^* is the carrier effective mass) and $1/\tau$ is the carrier scattering rate. The last two terms in Eq. 1 are the Lorentzian oscillators centered at ω_j , with the width γ_j and plasma frequency ω_{pj} . The best fits for 300, 80 and 10 K are shown in Fig. 3 with gray lines; the three individual components of Eq. 1 are shown with dashed lines. Table I summarizes the fitting parameters. We emphasize here that these parameters are unique, since no other values can reproduce the quality of the fits shown in Fig. 3.

As can be seen the scattering rate, $1/\tau$ monotonically decreases with decreasing temperature, whereas the plasma frequency of the Drude component is essentially temperature independent ($\omega_p \simeq 7,000 \text{ cm}^{-1}$). Such behavior is typical of conventional metals²¹⁻²³ and provides a strong argument against a HF state in Fe_2TiSn . Indeed the hallmark of the latter state is a strong increase of m^* below a temperature T^* characteristic of a given material. This is equivalent to a drastic reduction of the oscillator strength of the Drude component ($\omega_p^2 \sim 1/m^*$) (Ref. 14,15), which is not observed in our data.

Additional evidence against a HF state in Fe_2TiSn comes from the line-shape analysis of the $\sigma_1(\omega, T)$ spectra. The HF behavior has been shown before to leave characteristic fingerprints in the optical spectra of such systems (Ref. 14,15,24). Within a so called "hybridization scenario", hybridization between free carriers and localized f -electrons leads to a gap in the density of states that develops below the temperature T^* . Excitations across this hybridization gap, in addition to intraband absorption, give rise to the optical conductivity $\sigma_1(\omega)$ schematically shown in Fig. 4. At high temperatures ($T > T^*$), the conductivity of many HF systems follows a simple Drude response^{14,15,24} (thin solid line in Fig. 4). At $T < T^*$ two processes occur simultaneously: 1) the width of the Drude mode is collapsing so

that $1/\tau_2 \ll 1/\tau_1$, and 2) a finite frequency peak due to excitations across the hybridization gap appears. The latter contribution to $\sigma_1(\omega)$ shown in Fig. 4 was calculated within a BCS model with coherence factors type I (Ref. 15,25).

The $\sigma_1(\omega)$ data of Fe_2TiSn (Fig. 3) look qualitatively similar to the model spectra of Fig. 4: there is a Drude mode that narrows with temperature and a finite frequency peak at around 700 cm^{-1} . However, it appears that the temperature dependence of the latter excitation is completely uncorrelated with the Drude mode. Unlike HF systems, the spectral weight of the finite frequency peak ω_{p1} *decreases* slightly when lowering the temperature (Table I). Therefore, based on these findings one cannot interpret the 700 cm^{-1} peaks as being due to excitations across the hybridization gap. Instead we speculate that it is a low lying interband transition. A similar feature has not been seen in Fe_2VAL (Ref. 11); the data for Co_2TiSn does not extend low enough²⁷.

The absolute value of the Drude plasma frequency ω_p implies carrier density as small as $n \sim 5 \times 10^{20} \text{ cm}^{-3}$, under the assumption $m^* = m_0$ (m_0 is a free electron mass). This value of n is very similar to that found in both Co_2TiSn (Ref. 27) and Fe_2VAL (Ref. 11,28). It is striking that even though the carrier density is essentially the same in Fe_2TiSn and Fe_2VAL , the former compound shows metallic, whereas the latter displays an insulating temperature dependence of the dc resistivity. This indicates that localization (probably due to disorder) plays an important role in the charge dynamics. For Fe_2TiSn , we estimate the carrier mean free path $l \simeq 80 \text{ \AA}$ at room temperature. Such a long mean free path signals that, unlike Fe_2VAL (Ref. 28), the Boltzmann formalism should still hold for Fe_2TiSn .

In addition to the free electron Drude component and a low-lying transition at 700 cm^{-1} , the optical spectrum of Fe_2TiSn exhibits another excitation at around $7,000 \text{ cm}^{-1}$ (Fig. 3 and Tab. I). A similar peak at $7,000 \text{ cm}^{-1}$ has been seen before in Fe_2VAL (Ref. 11). This is not unexpected, however, as the band structure calculations for both compounds show that the bands around the Fermi level are predominantly coming from Fe d -orbitals^{7-10,12}. In Fe_2VAL , the $7,000 \text{ cm}^{-1}$ peak has been interpreted as being due to excitations across a pseudogap¹¹. The band structure calculations for Fe_2TiSn (Ref. 12,29) have also predicted the existence of a partial gap (pseudogap) at the Fermi level of about 0.5 eV. Although the position of the peak in Fe_2TiSn does not exactly agree with this predicted value, we believe that it can be interpreted as being due to excitations across such a gap. Namely the magnitude of the gap has been shown before to depend strongly on atomic disorder²⁹, which is difficult to control during sample growth.

In conclusion, our IR results do not support the notion that the Kondo interaction plays a dominant role in the charge dynamics of Fe_2TiSn . We find that the effective mass of free carriers is essentially temperature independent. By analogy with Fe_2VAL , we suggest that

the apparent mass enhancement at low temperatures is due to a Schottky anomaly arising from magnetic clusters. The latter effect can also explain the anomalous temperature dependence of specific heat and dc resistivity at low temperatures. The free electron contribution to the optical conductivity of Fe₂TiSn appears to be conventional Drude-like, with a small carrier density and relatively long mean free path. The interband transition at 7,000 cm⁻¹ can be interpreted as excitations across a pseudogap predicted in band structure calculations.

We thank E.J. Singley for useful discussions. The research at UCSD supported by DOE, NSF and the Research Corporation.

** Also at Institute of Physics, University of Silesia, 40-007 Katowice, Poland

¹ O. Heusler, *Ann.Phys.* **19**, 155 (1934).
² Y. Fujita, K. Endo, M. Terada and R. Ikamura, *J.Phys.Chem.Solids* **33**, 1443 (1972).
³ F.B. Mancoff, B.M. Clemens, E.J. Singley and D.N. Basov, *Phys.Rev.B* **60**, 12565 (1999).
⁴ L. Degiorgi, A.V. Sologubenko, H.R. Ott, F. Drymiotis and Z. Fisk, *Phys.Rev.B* **65**, 041101(R) (2002).
⁵ Y. Nishino, M. Kato, S. Asano, K. Soda, M. Hayasaki, U. Mizutani, *Phys.Rev.Lett.* **79**, 1909 (1997).
⁶ C.S. Lue, J.H. Ross Jr., C.F. Chang and H.D. Yang, *Phys.Rev.B* **60**, 13941 (1999).
⁷ R. Weht, and W.E. Pickett, *Phys.Rev.B* **58**, 6855 (1998).
⁸ D.J. Singh, and I.I. Mazin, *Phys.Rev.B* **57**, 14352 (1998).
⁹ M. Weinert, and R.E. Watson, *Phys.Rev.B* **58**, 9732 (1998).
¹⁰ G.Y. Guo, G.A. Botton, and Y. Nishino, *J.Phys.Cond.Mat.* **10**, L119 (1998).
¹¹ H. Okamura, J. Kawahara, T. Nanba, S. Kimura, K. Soda, U. Mizutani, Y. Nishino, M. Kato, I. Shimoyama, H. Miura, K. Fukui, K. Nakagawa, H. Nakagawa and T. Kinoshita, *Phys.Rev.Lett.* **84**, 3674 (2000).
¹² A. Slebarski, M.B. Maple, E.J. Freeman, C. Sirvent, D. Tworuszka, M. Orzechowska, A. Wrona, A. Jezierski, S. Chiuzaibaian, M. Neumann, M., *Phys.Rev.B* **62**, 3296 (2000).
¹³ A. Slebarski, M.B. Maple, A. Wrona, A. Winiarska, *Phys.Rev.B* **63**, 214416 (2001).
¹⁴ L. Degiorgi, *Rev.Mod.Phys.* **71**, 687 (1999).
¹⁵ S.V. Dordevic, D.N. Basov, N.R. Dilley, E.D. Bauer, M.B. Maple, *Phys.Rev.Lett* **86**, 684 (2001).
¹⁶ P. Wachter, in *Handbook on the Physics and Chemistry of Rare Earths*, Vol. **19**, edited by K.A.Gschneidner and LeRoy Eyring, (Elsevier Science, Amsterdam, New York, 1994).
¹⁷ S. Donovan, A. Schwartz, and G. Gruner, *Phys.Rev.Lett* **79**, 1401 (1997).
¹⁸ P.E. Sulewski, A.J. Sievers, M.B. Maple, M.S. Torikachvili, J.L. Smith, and Z. Fisk, *Phys.Rev.B* **38**, 5338 (1988).

¹⁹ C. Homes, M.A. Reedyk, D.A. Crandels and T. Timusk, *Applied Optics* **32**, 2976 (1993).
²⁰ We did not attempt to fit the phonon mode at 250 cm⁻¹.
²¹ F. Wooten, *Optical Properties of Solids*, (Academic Press, New York, 1972).
²² E. Fawcett, *Rev.Mod.Phys.* **60**, 209 (1988).
²³ S.V. Dordevic, D.N. Basov, R.C. Dynes and E. Bucher, *Phys.Rev.B* **64**, 161103 (2001).
²⁴ L. Degiorgi, F.B.B. Anders, G. Gruner, *European Physical Journal B*, **19**, 167 (2001).
²⁵ We have performed a calculation of $[\sigma_1(\omega, T < T^*)/\sigma_1(\omega, T > T^*)]$, the ratio of the optical conductivity below and above the coherence temperature. The method follows closely the BCS calculation²⁶, except that the coherence factors are of type I, as opposed to type II in conventional superconductors.
²⁶ M. Tinkham, *Introduction to Superconductivity*, Second Edition, (McGraw-Hill, New York, 1996).
²⁷ E.I. Shreder, M.M. Kirillova, V.P. Dyakina, *Physics of Metals and Metallography* **90**, 362 (2000).
²⁸ Y. Feng; J.Y. Rhee, T.A. Wiener, D.W. Lynch, B.E. Hubbard, A.J. Sievers, D.L. Schlage, T.A. Lograsso, L.L. Miller, *Phys.Rev.B* **63**, 165109 (2001).
²⁹ A. Jezierski, and A. Slebarski, *J.Magn.Magn.Mat* **223**, 33 (2001).

FIG. 1. The reflectance data of Fe₂TiSn at 10, 80 and 300 K. The spectra show anomalous temperature dependence in the mid-infrared range.

FIG. 2. The optical conductivity $\sigma_1(\omega)$ of Fe₂TiSn is characterized by a narrow Drude mode and an interband transitions at around 7,000 cm⁻¹. A strong peak at 250 cm⁻¹ is an optically active phonon mode.

FIG. 3. Drude-Lorentz fits of the optical conductivity $\sigma_1(\omega)$ at 300, 80 and 10 K. As temperature decreases the Drude peak narrows, but its spectral weight appears to be conserved. The 7,000 cm⁻¹ peak is only weakly temperature dependent.

FIG. 4. Schematic behavior of the frequency dependent optical conductivity $\sigma_1(\omega)$ in an *f*-electron HF system. Note that below T* both $1/\tau$ and ω_p of the Drude mode are strongly reduced.

TABLE I. Fitting parameters from Eq. 1, with all the values given in the units of cm⁻¹.

	ω_p	$1/\tau$	ω_{j1}	γ_1	ω_{p1}	ω_{j2}	γ_2	ω_{p2}
10 K	7,100	120	600	2,000	12,250	6,800	21,000	71,700
80 K	7,200	150	600	2,000	12,250	6,800	21,000	71,700
300 K	6,870	200	700	2,000	14,000	7,000	21,000	71,700

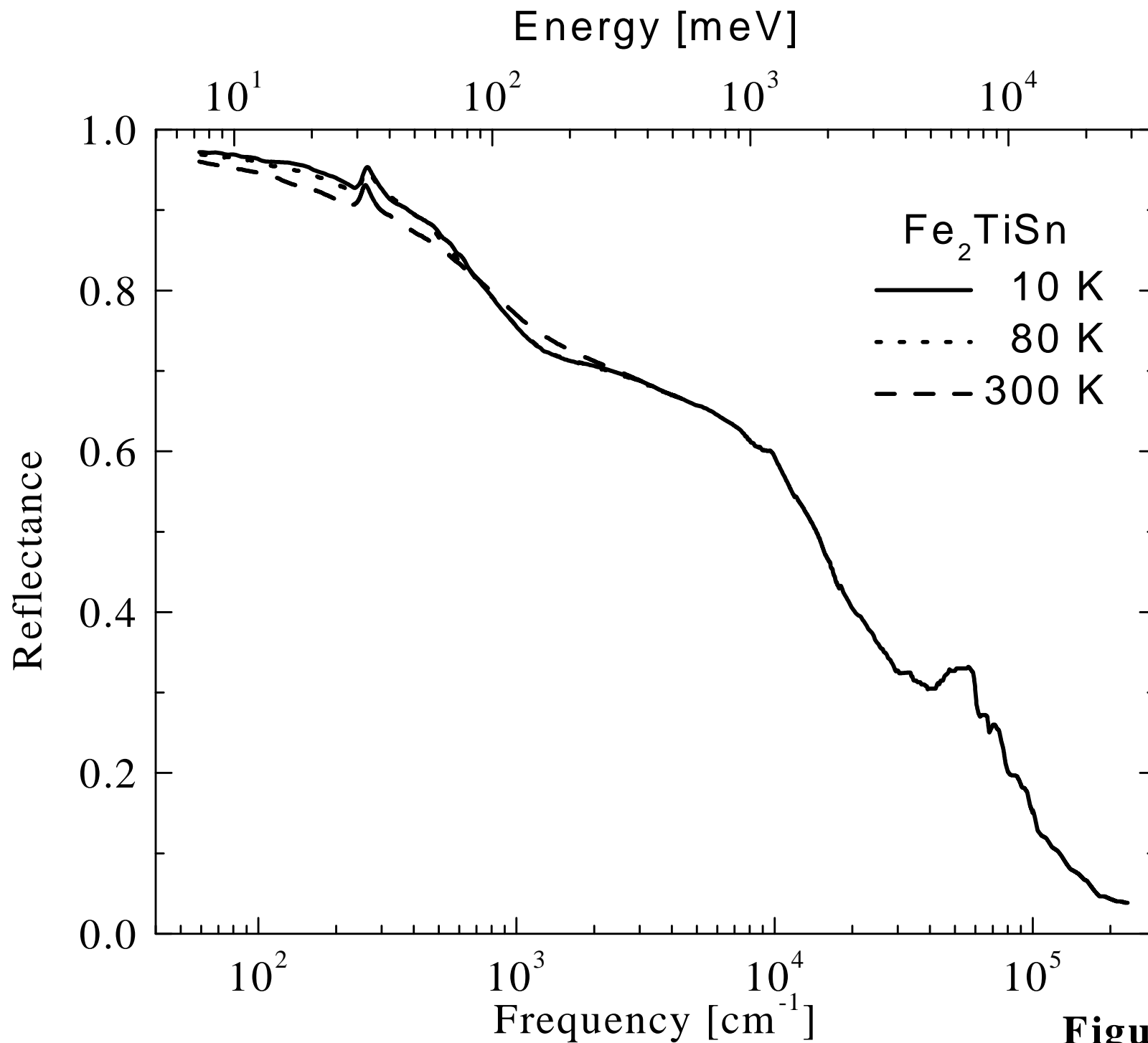


Figure 1

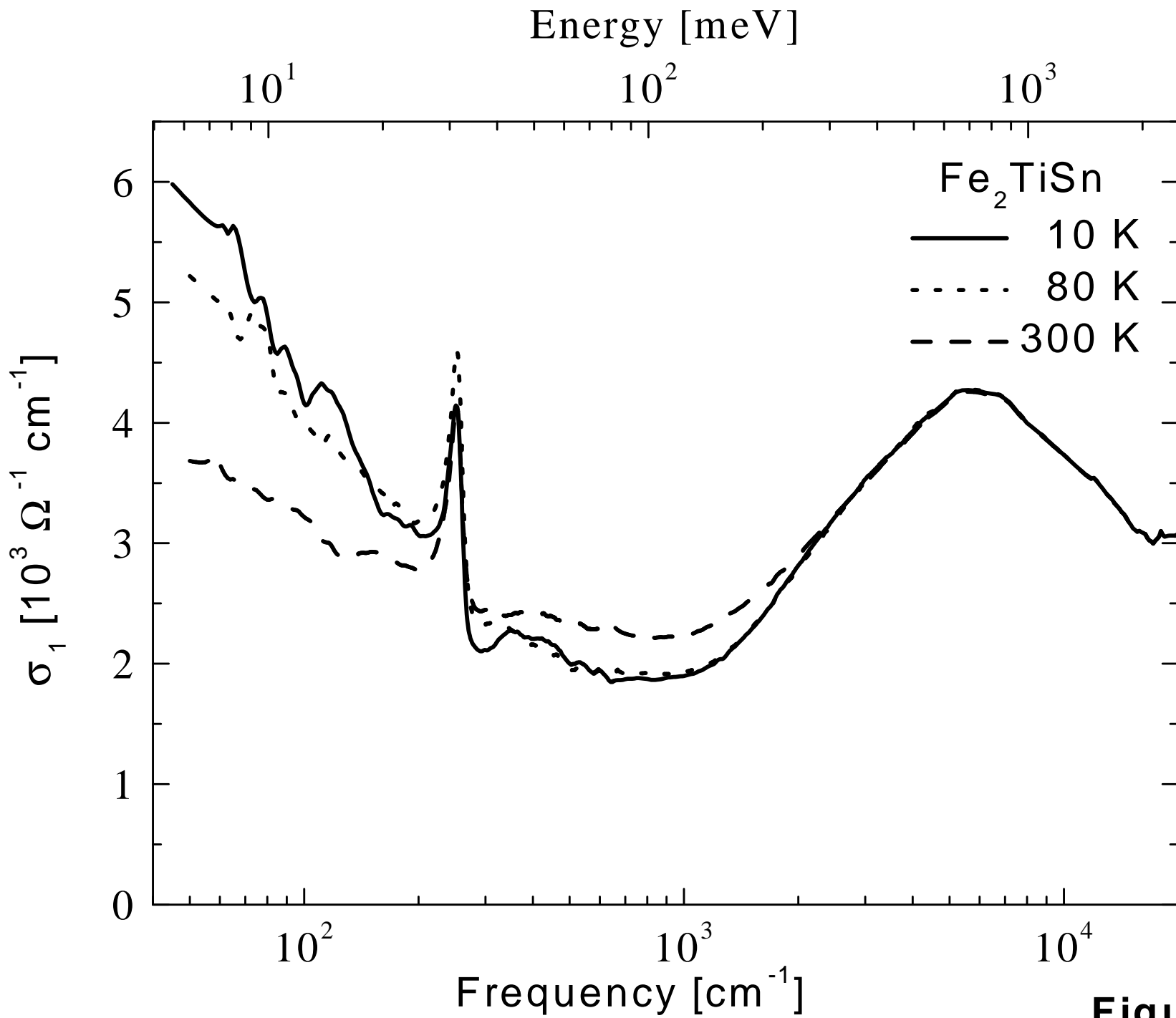


Figure 2

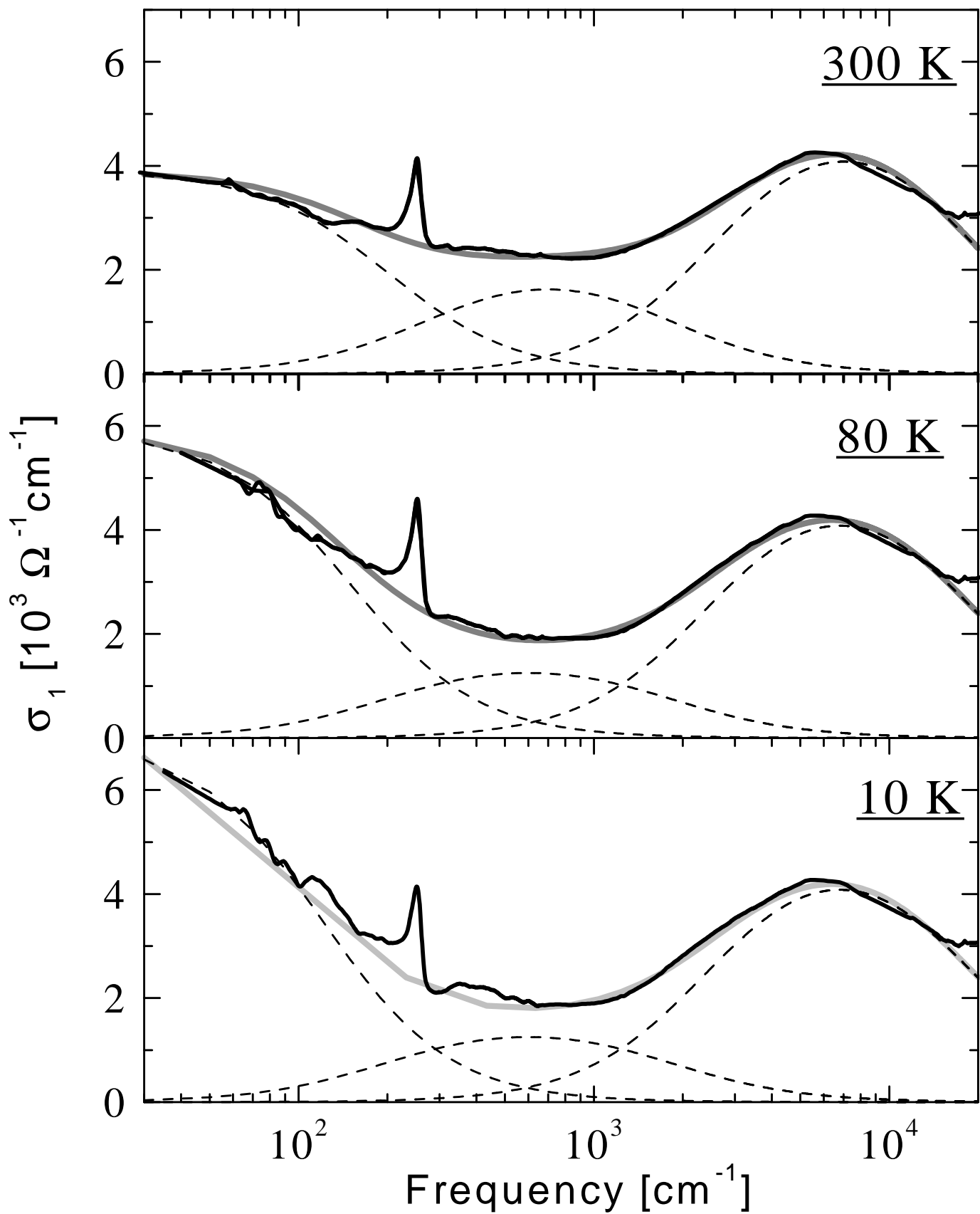


Figure 3

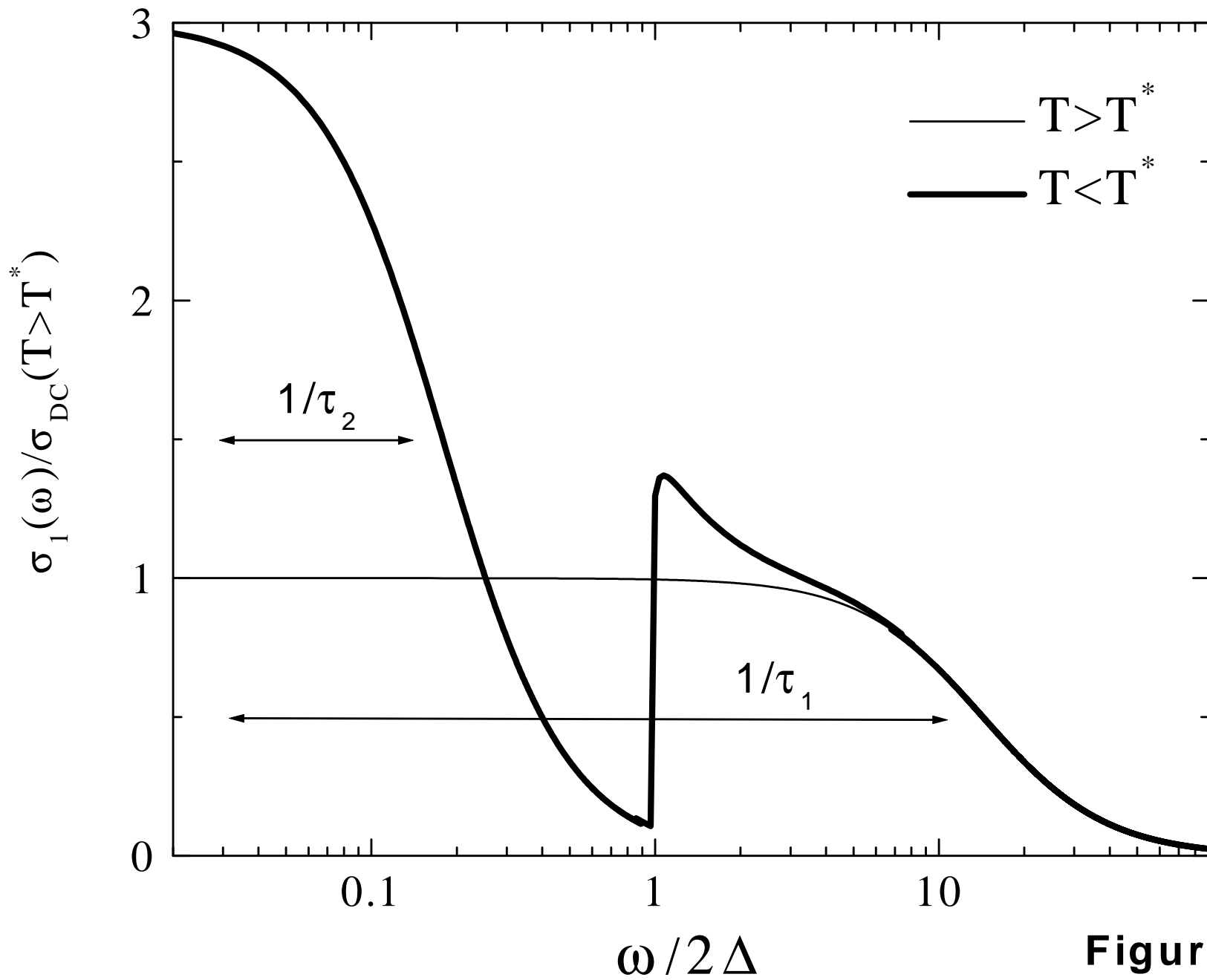


Figure 4